Journal of Petroleum Science and Technology 13(1): 37, 2023, Pages 49-58
DOI:10.22078/jpst.2023.5197.1894

Journal of Petroleum Science and Technology
Research Paper
https://jpst.ripi.ir/

The Effect of Monovalent Ions on the Oil/Brine Electrical Behavior Using a Novel Surface Complexation Model

Hamed Farhadi
Department of Chemical and Petroleum Engineering, Sharif University of Technology, Tehran, Iran

Abstract
Oil/brine electrical behavior could control the wettability of the oil/brine/rock system during low salinity water flooding. However, there is a lack of understanding of chemical reactions occurring on the oil surface. There are a few surface complexation models (SCMs) for the oil/brine interface, and all of them assume that the surface site density is a fixed number, like the mineral surface. The current study assessed two existing models on this subject (Model A and B). These models ignore the dynamic nature of the oil/brine interface. Therefore, they failed to capture experimentally measured ζ potentials appropriately. Therefore, this study constructed a novel diffuse layer SCM (Model C) considering the interfacial concentration of surface carboxylic acid as a function of brine salinity for each salt, including NaCl, Na_2SO_4, $CaCl_2$, $MgCl_2$, and $NaHCO_3$. Model C matches the experimental data of the literature far better than A and B. Based on Model C, Na^+, Cl^-, and SO_4^{2-} cannot be adsorbed on the oil/brine interface; however, the role of these ions in the electrical behavior of crude oil/brine is only to affect the interfacial concentration of -COOH. For example, an increase in Na+ reduced the oil/brine IFT. Therefore, more carboxylic groups would be available at the oil/brine interface. As a result, $-COO^-$ concentration increases, and the crude oil surface becomes more negatively charged. The current study indicated that Ca^{2+} and Mg^{2+} are not the only factors that make the interface more positively charged. However, an increase in IFT (in this study by salinity reduction) significantly makes the oil/brine interface more positive, too.

Keywords: Surface Chemistry, Complexation Model, Interfacial Tension, Zeta Potential.

Introduction
Low salinity water flooding (LSWF) re-establishes the thermodynamic equilibrium of oil/brine/rock system to enhance oil recovery of oil/brine/rock system [1–5]. It has been shown that low salinity water flooding has a great potential to be selected as an EOR method [6–8]. Wettability change toward a more water-wet state is widely accepted as a primary mechanism of improved oil recovery during LSWF [9–13]. The wettability alteration occurs when a thicker water film is created on the rock surface [14–16]. The attractive and repulsive forces between oil/brine and rock/brine interfaces control the thickness of the water film [17,18]. Attractive Van der Waals and attractive/repulsive electrostatic forces are dominant forces [9,19]. The latter depends on the sign of the electric charges at two interfaces. The range of variation in electrical potential of oil/brine versus salinity is greater than that of brine/rock interface, particularly in carbonate reservoirs [20,21]. Therefore, the electrical behavior of the oil/brine interface is of greater significance in improving the chance of the success of LSWF.

Although considerable efforts have been put into studying carbonate rock/brine interface by measuring zeta (ζ) potential, a few researchers investigated the electrical behavior of oil/brine surface [22]. The ζ potential, the electric potential at the shear plane, is the most common method to quantify the electrical properties of the oil/brine interface [17,23]. Kolltveit et al. [24] investigated the electrical behavior of three crude oil samples with NaCl brines by measuring ζ potential at different salinity and pH. They found that brine salinity increased the ζ potential of all crude oil droplets in brines. However, their results didn't reveal any relation between the measured ζ potential and pH. Mahmoudzadeh et al. [25] and Farhadi et al. [20] measured the oil/brine ζ potential at different seawater salinities. Based on the results, further brine dilution from a certain brine salinity leads to a rise in the ζ potential. In another work, the ζ potential of crude oil emulsion in different single brines (including NaCl, NaOH, $MgCl_2$, and $CaCl_2$) was measured and modeled by Takeya et al. [23]. They concluded that the reduction

*Corresponding author: Hamed Farhadi, Department of Chemical and Petroleum Engineering, Sharif University of Technology, Tehran, Iran
E-mail addresses: hamed.farhadi88@gmail.com
Received 2023-07-25, Received in revised form 2023-10-28, Accepted 2023-11-05, Available online .....

in ζ potential due to salinity reduction is a result of the electrical double layer (EDL) expansion. Farhadi et al. [22] recently revealed that the EDL expansion is not the only reason behind the reduction in the ζ potential with brine dilution. They discovered that the density of -COOH sites is a function of brine salinity/composition, and the variable site density significantly affects the ζ potential. The absence of clear insight into the effect of brine pH, salinity, and composition on the electrical behavior of the oil/brine interface is the motive of the present study to develop a new surface complexation model (SCM) that can explain the complexity of the oil surface.

An SCM simulates the chemical equilibrium based on chemical reactions at the oil/brine interface. Using an SCM as an alternative to the experimental methods helps to understand the electrical properties of the oil surface. Brady et al. [26] developed a diffuse layer model with (-COOH) and (-NH) sites at the oil/brine interface to simulate the electrical properties of the oil surface. In their model, the base sites can only develop a positively charged surface by protonation. However, the acid sites make the surface negatively or positively charged by dissociation or divalent cation adsorption. However, the monovalent ions were neutral to the surface charge since they assumed these ions do not adsorb on the defined sites. Qiao et al. [27,28] constructed a surface complexation model for the oil/brine system to model oil recovery from a core during LSWF. They assumed that only carboxylic groups (-COOH) are present at the oil/brine interface and assigned a specific surface site density to each crude oil based on its acid number (AN). Takeya et al. [29] investigated different crude oil surfaces using a combination of experimental ζ potential measurements and a triple-layer surface complexation model. They found that the site density of (-COOH) has a linear correlation with the resin content in crude oil and a logarithmic relationship with the AN content of crude oil. In addition, Bonto et al. [30] developed an SCM considering the chemistry of different oils by taking surface site density as a linear function of the acid and base numbers. They tuned the obtained surface site density based on the ζ potentials reported in the literature. In the developed SCM, Na^+ can be adsorbed to the oil surface. All the reviewed SCM models assumed that the oil surface site density was constant even with changing brine pH, salinity, and composition. They did not consider the acid and base group distribution changes at the oil/brine interface under different conditions. Also, there is no consensus on the adsorption of monovalent on the oil surface.

It is well-established that the surface site density of mineral surfaces is constant. The electrical behavior of the mineral/brine interface is a function of salinity, composition, and pH [15,31–34]. The theory of constant surface site density has also been implemented on the oil surface [30] to develop a surface complexation model for the oil/brine interface. In other words, in the prediction of the electrical behavior of the oil surface, the effect of adsorption of surface active agents from the oil bulk into the oil/brine interface is overlooked. Measuring the interfacial dilatation rheology, Freer and Radke [35,36] indicated that asphaltene molecules transport from the oil bulk to the oil/brine interface. In addition, Spiecker and Kilpatrick [37] performed interfacial shear rheometry tests to investigate the role of asphaltene molecules on the interfacial behavior of the oil/brine system. They revealed that an asphaltenic film forms at the oil/brine interface, and the asphaltene accumulation in this film depends on the heavy metal content, polarity, and aromaticity. Recently, it was indicated that the adsorption of surface active agents onto oil/brine surface is also dependent on brine salinity [24,38,39]. Therefore, considering the role of brine chemistry and its interaction with oil surface-active components helps to perceive the electrical behavior of the oil surface. Hence, this work developed a diffuse-layer SCM considering the impact of brine pH, salinity, and composition on the surface site density of oil surface and its electrical behavior. Using density functional theory (DFT), Andersson et al. [40] indicated that it is more favorable for acid and base materials to accumulate at the oil/brine interface than the oil bulk. In other words, the total acid and base numbers of crude oil are the indexes of the surface density site of these surface active agents at the oil/brine interface. By analyzing Fourier transform ion cyclotron resonance (FT-ICR) mass spectrometry data, Jan Czarnecki [41] revealed that the composition of accumulated materials at the oil/brine interface differs from asphaltene and resin of the oil bulk. Yang et al. [42] sub-fractioned the asphaltene molecules based on their interfacial activity. They showed that less than 2% of asphaltene molecules are responsible for interfacial properties. In another study, using experimental findings and molecular dynamic simulation, Yang et al. [43] showed that sub-fraction of asphaltene with higher molecular weight and higher content of heteroatoms (e.g., oxygen) were more engaged in crude oil/brine surface. It can be concluded that total acid/base numbers are not a befitting representative for surface active material or surface site density of the oil/brine interface. However, interfacial tension (IFT) between oil and brine is an adequate index for accumulating surface-active materials at the oil/brine interface. Thus, in this work, IFT was used as an index of the level of transportation of acid/base materials to the oil/brine interface and the oil surface site density. Figure 1 shows a schematic representation of the relation between the oil/brie IFT and the surface site density of oil. As shown in Figure 1, at high IFT condition (Fig. 1-Left), most surface-active molecules reside inside the oil bulk. Changing brine to achieve a low IFT condition (Figure 1-Right) causes the surface-active molecules to travel into the oil/brine interface.

The presented literature lacks an SCM that considers the fluid nature of oil instead of handling its surface as a solid. Therefore, this study developed a novel diffuse-layer SCM considering the interfacial concentration of the -COOH group as a function of brine salinity and composition. The model is validated by fitting the experimental ζ potential of the oil/brine interface under different conditions reported in the literature. The model is either as good as or outperforms the previous models in the whole range of brine salinity and composition. To develop such a model, the oil/brine IFT is set as the index to characterize the transport of surface-active material from the oil bulk to the interface and to determine -COOH site density at different salinity and composition. A new concept is developed for surface chemistry and the issue of the adsorption of monovalent ions such as Na is addressed using the new model.

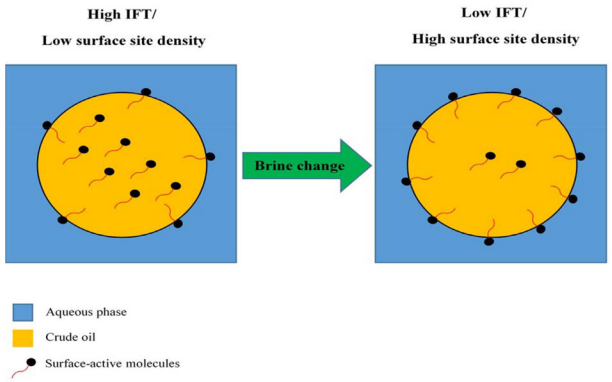

Fig. 1. Relation between the oil/brine IFT and the accumulation of surface-active materials at the oil surface with changing brine.

Materials and Methods

The existing surface complexation models, describing the electrical properties of the oil/brine interface, consider that the surface site density is always constant, even with a change in brine salinity and composition [44,45]. The issue was addressed by calculating the surface site density based on the acid and base content of oil and the IFT behavior of the oil/brine system.

Surface Complexation Model

Step 1: Determining Surface Site Density as a Function of the Oil/Brine IFT

This study uses the oil/brine IFT as an index to describe the concentration of surface-active materials at the oil/brine interface. Farhadi et al. [39] developed a mathematical model (see Eq. (1)) based on the drift-diffusion theory to describe the transport of polar molecules from the oil bulk to the interface.

$$\gamma(t) = \gamma_0 - A\sqrt{Dt} \quad (1)$$

where γ(t) is time-dependent interfacial tension (mN/m), γ_0 is interfacial tension at the beginning of the oil drop formation (mN/m), A is a constant depending on the oil composition, D is the diffusion coefficient of polar molecule from oil bulk to the interface ($m^2.s^{-1}$), and t is time (s). Brine salinity and composition could change the oil/brine IFT [39,46–48]. The oil/brine IFT reaches equilibrium, giving enough time at t_{eq}. In the current study, to simplify the physics of the problem, it is assumed that t_{eq} is the same for all brines. For the desired brine (denoted by "x") and the brine with minimum IFT (denoted by "min"), at the equilibrium condition, Eq. (1) is rewritten in the form of Eqs. (2) and (3), respectively.

$$\gamma_0-\gamma_x(t_{eq}) = A\sqrt{(D_x\, t_{eq})} \quad (2)$$

$$\gamma_0-\gamma_{min}(t_{eq}) = A\sqrt{(D_{max}\, t_{eq})} \quad (3)$$

Eq. (4) is derived by dividing Eq. (3) by Eq. (2):

$$\frac{\gamma_0-\gamma_{min}(t_{eq})}{\gamma_0-\gamma_x(t_eq)} = \frac{\sqrt{D_{max}}}{\sqrt{D_x}} \Rightarrow \frac{D_x}{D_{max}} = \left(\frac{\gamma_0-\gamma_x(t_eq)}{\gamma_0-\gamma_{min}(t_{eq})}\right)^2 \quad (4)$$

The ratio of the diffusion coefficient of polar molecules (D_x/D_{max}), equals the ratio of the concentration of surface-active material at the interface (or the ratio of total surface site density). In other words, the total surface site density for the desired brine can be obtained by Eq. (5):

$$N_{-COOH}+N_{-NH})_x = (N_{-COOH}+N_{-NH})_{max} \times \left(\frac{\gamma_0-\gamma_x(t_{eq})}{\gamma_0-\gamma_{min}(t_{eq})}\right)^2 \quad (5)$$

where N_{-COOH} and N_{-NH} denote the density of -COOH (carboxylic acid) and -NH (Ammonium) groups at the oil surface. Therefore, to obtain the surface site density of the desired brine, one should first estimate the maximum surface site density.

Eftekhari et al.[49] thermodynamically obtained the acid (N_{-COOH}) and base (N-NH) site density using total acid and base numbers, respectively [49].

$$N_{-COOH} = 0.602\times10^6 \frac{TAN}{1000\, a_{oil}\times MW_{KOH}} \quad (6)$$

$$N_{-NH} = 0.602\times10^6 \frac{TBN}{1000\, a_{oil}\times MW_{KOH}} \quad (7)$$

where 0.602×10^6 is the conversion factor from mol/m^2 to $\#/nm^2$, TAN is the total acid number (mg KOH/g oil), TBN is the total base number (mg KOH/g oil), aoil is the specific area of oil (m^2/g), and MWKOH is the molecular weight of KOH. In the current study, the oil drop was assumed spherical with a diameter of 1 μm; therefore, the specific surface area of oil is 6.88 m^2/g. Eftekhari et al.[49] assumed all the oil bulk's acid and base molecules are present at the interface. However, only a fraction of the acid and base groups can be surface-active material. Bonto et al. [44] corrected Eqs. (6) and (7) to apply the mentioned concept based on the previous experimental evidence (see Eqs. (8) and (9)):

$$N_{COOH\,max} = 0.5+0.678(N_{COOH}-0.05) \quad (8)$$

$$N_{NH\,max} = 2/3\, N_{NH} \quad (9)$$

The total surface site density versus brine salinity/composition can be predicted by inserting $N_{COOH\,max}$ and $N_{NH\,max}$ (obtained from Eqs. (8) and (9), respectively) into Eq. (5). Then, based on the pH condition one can roughly estimate the amount of $N_{COOH\,x}$ and $N_{NH\,x}$ separately.

Measuring the ζ potential of oil/bine in different pH and salinity values, Buckley et al. [50] indicated that base groups affect the interface electrical properties only at very low pH. Nenningsland et al. [51] also stated that the travel of the base group from the oil bulk to the interface is negligible at pHs larger than 4. At pH values above 4, carboxylic dissociation dominates the crude oil/brine IFT behavior. Bertheussen et al. [52] showed that the transport of base groups to the interface is a function of their molecular weight, in which the high molecular weight bases (dominant species in crude oil samples) do not significantly partition into the aqueous phase. However, high and low molecular weight acid groups partition into the aqueous phase at pHs higher than 5. Also, Farhadi et al. [39] showed that the IFT behavior of crude oil/brine originated from carboxylic acid groups, which agrees with other studies [48,53–55]. Therefore, this study assumes that the -NH density is a constant value and rewrites Eq. (5) as follows:

$$N_{-COOH\,x} = N_{-COOH\,max} \times \left(\frac{\gamma_0-\gamma_x(t_{eq})}{\gamma_0-\gamma_{min}(t_{eq})}\right)^2 \quad (10)$$

Eq. (10) determines the -COOH site density for the crude oil in contact with a brine sample. As stated before, γ_0 is the IFT between oil and brine when they first come into contact. For every oil sample, the IFT is the largest value since no surface-active molecules have yet traveled from the oil bulk to the interface. Usually, dynamic IFT (the IFT vs. time) is not an available experimental data; therefore, γ_0 is set as a matching parameter (based on the experimental ζ potential), which should be higher than the largest measured equilibrium IFT. Also, γ_{min} is the minimum IFT related to a state in which all surface-active molecules of oil bulk travel to the interface.

This parameter was also considered a matching parameter (based on the experimental ζ potential), constrained by the smallest measured equilibrium IFT. Finally, γ_x or IFT should be specified for each salinity, and composition. The IFT data were extracted for each oil and described in Appendix A.

Step 2: Defining the Surface Reactions

After determining the oil surface properties, a diffuse double-layer surface complexation model was implemented in PHREEQC V.03 to estimate the oil surface potential. PHREEQC is a geochemical modeling software based on the C++ programming language. To generate the diagrams of this study, IPhreeqcCOM-3.7.3-15968 was coupled with MATLAB software. This coupling expedited the diagram generation and didn't change the outcomes of PHREEQC V.03. to Reactions 1-4 (see Table 1) and their equilibrium constants are taken from Brady et al.[56]. Reactions 5-9 (see Table 1), which consider weak bonds and Na adsorption, are taken from Bonto et al.[44]. The current study introduces reactions 8-10 (see Table 1) that have the same stoichiometry and equilibrium constants as reactions 2-4; however, the sign ">>" states that carboxylic acid groups have a variable surface site density with changing brine salinity/composition based on Eq. (10). Table 1 introduces three models to compare the novel model of this study (Model C) with previous models (models A and B). Model A assumes that carboxylic acid groups have a constant surface density [56]. Model B adds surface reactions of weak bonds and Na adsorption to Model A [44]. Model C manipulates Model A by considering the change in the surface site density of carboxylic acid groups with brine salinity/composition.

The total base number of all crude oil samples used in this study was unknown. Therefore, the Surface site density of ammonium groups (-NH) was considered a matching parameter. The value of this parameter is reported in Table 2. The total acid number of all crude oil samples used in this study was available. Therefore, the surface site density of carboxylic acid groups for Model A and Model B is estimated through Eq. (8). The surface site density of carboxylic acid groups for Model C is obtained from Eq. (10).

Surface charge (σ_S) was obtained by subtraction of the total mole of positive surface species (such as $-NH^+$, $-CO_3Ca^+$, $-CO_3Mg^+$) from that of negative surface species (such as $-COO^-$) as follows:

$$\sigma_s = \frac{F}{AS}\left(\sum m_{pi} - \sum m_{ni}\right) \quad (11)$$

where F is Faraday constant (96485 C/mol), A is specific surface area (m^2/g), S is the amount of oil distributed in brine (g/L), m_{pi} is the mole of ith positive surface complex (mol/m^2), and m_{ni} is the mole of i^{th} negative surface complex (mol/m^2). Then, the surface potential (ψ) was related to the surface charge using Grahameh Eq., derived from Gouy-Chapman model [57].

$$\sigma_s^2 = 8000\varepsilon\varepsilon_0 RTI\left(\sinh\left(\frac{ZF\psi}{2RT}\right)\right)^2 \quad (12)$$

Table 1 The surface reaction of crude oil and water species and their equilibrium constant.

#	Surface reaction	Log K Model A	Log KModel B	Log K Model C
1		6.00	7.27	6.00
2		-4.80	-4.65	0
3		-3.80	-3.30	0
4		-4.00	-3.30	0
5		0	-3.40	0
6		0	-6.23	0
7		0	-4.60	0
8		0	-4.60	0
9		0	-5.70	0
10		0	0	-4.80
11		0	0	-3.80
12		0	0	-4.00

Table 2 The matched parameters of different models used in this work.

Oil type	(mN/m)	(mN/m)	-NH (#/m²)Model A	-NH (#/m²)Model B	-NH (#/m²) Model C	x (nm) Model A	x (nm) Model B	x (nm) Model C
Crude oil I [65]	22	3.8	0.05	0.05	0.05	0.6	0.6	0.3
Crude oil II [20,25]	21.4	5.5	0.05	0.05	0.05	0.3	0.3	0.3

where ε is the dielectric constant of pure water, ε_0 is the vacuum permittivity (8.854×10^{-2} F/m), T is the absolute temperature (298.5 K in this study), R is the constant of the ideal gas (8.314 J/(mol.K)), I is the brine ionic strength (M), and Z is the charge of a symmetric electrolyte sample.

Step 3: ζ Potential Determination

Using the obtained surface potential, we calculated the ζ potential using the Gouy-Chapman Eq. (see Eq. (13)).

$$\psi(x)=\frac{2K_BT}{e}\ln\left(\frac{1+\gamma e^{-kx}}{1-\gamma e^{-kx}}\right) \quad (13)$$

where

$$\gamma=\frac{e^{\frac{\psi r_0}{2}}-1}{e^{\frac{\psi r_0}{2}}+1} \quad (14)$$

where ψ_{r0} is the reduced surface potential as follows:

$$\psi r_0=\frac{e\psi_0}{K_BT} \quad (15)$$

where ψ_0 is the surface potential, k_B is the Boltzmann constant (1.38064852×10^{-23} $m^2kgs^{-2}K^{-1}$), e is the charge of an electron (1.60217662×10^{-19} C), T is the absolute temperature (K), and x is the distance of shear plane (where ζ potential is assumed to be measured [58]) with the crude-oil surface. The shear plane lies near the outer Helmholtz plane (OHP); however, there is not a clear understanding of the distance of the shear plane from this surface [58,59]. Literature has reported different values for shear plane location, i.e., 0.33 nm [60,61], 0.6 nm [50,62,63], and 2 nm [64]. Therefore, the current study assumed that the distance between the oil surface and shear plane for each crude oil sample is a matching parameter between 0.3 and 0.6 nm (based on the experimental ζ potential). The matched values of x are reported in Table 2.

Step 4: Validation

The final step is to assess the performance of the models presented in Table 1. Therefore, we compare the calculated ζ potential for each model with the ζ potential values of the literature. A few experimental works have studied the oil/brine ζ potential. Fewer of these works measured the ζ potential and the IFT of crude oil/brine simultaneously, which are as follows:

1- Farhadi et al. [65] measured the ζ potential and the IFT of crude oil I/single-salt brines (including NaCl, $CaCl_2$, $MgCl_2$, Na_2SO_4, and $NaHCO_3$) in a wide range of salinity.

2- Mahmoudzadeh et al. [25] and Farhadi et al. [12] used the same crude oil (named crude oil II) to measure the ζ potential at different salinity levels of Persian Gulf seawater.

The matching parameters for the mentioned oils are listed in Table 2.

Results and Discussion

The Effect of Ionic Strength on Single Salt Brine

Farhadi et al. [65] measured the IFT and ζ potential of crude oil in contact with different single salt brines, including NaCl, Na_2SO_4, $NaHCO_3$, $CaCl_2$, and $MgCl_2$. They provided experimental evidence on the impact of the crude oil/brine IFT on the role of individual ions (such as Na, Ca, and Mg) in the electrical behavior of the crude oil surface.

Na^+ Concentration

The results of ζ potential predictions of each of the surface complexation models, described in Table 1, were plotted against the experimental results of Farhadi et al. [24] for NaCl and Na_2SO_4 brines. As shown in Fig. 2, neither Model A nor Model B can predict the general relation between the crude oil/brine ζ potential and ionic strength. Model C, the novel model presented in this study, can match the experimental data in trend and value.

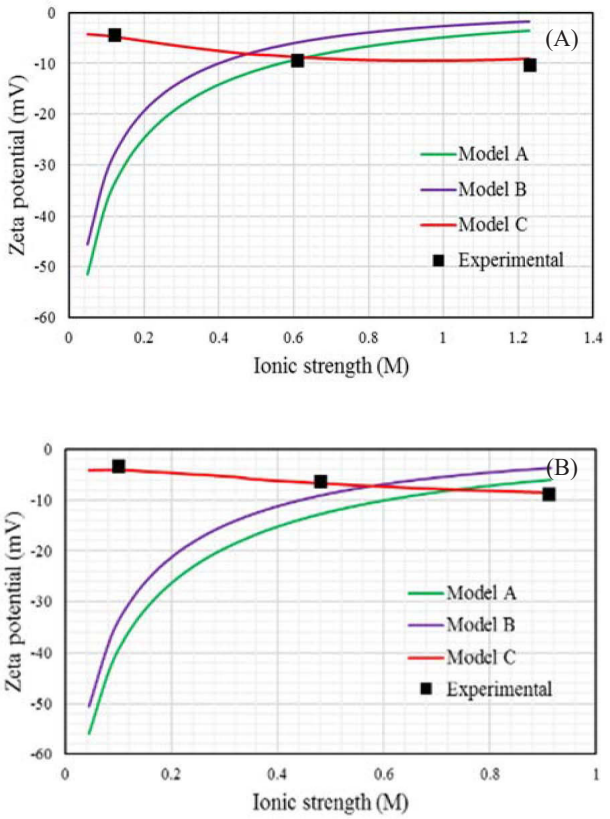

Fig. 2 ζ potential of crude oil I/brine at different salinity levels for a) NaCl brine and b) Na_2SO_4 brine.

Model A assumes that the surface site density is constant. Also, based on Table 1, Model A does not consider Na or Cl adsorption on the surface. Therefore, based on Model A, a decrease in the ionic strength in an almost fixed pH reduces the ζ potential due to EDL expansion. Model B considers the effect of Na^+ ions by Na adsorption on the crude oil surface. Hence, based on Model B, a reduction in the ionic strength decreases the ζ potential due to EDL expansion and less Na adsorption. Fundamentally, none of these two models can predict the increase in the ζ potential with salinity reduction. However, Model C predicts the experimental data by considering the variation in -COOH density as a function of the IFT behavior.

Since the change in IFT and ζ potential for NaCl and Na_2SO_4 are similar, we selected NaCl brine for more investigation. Figure 3 shows the concentration of surface species formed at the crude oil/NaCl brine interface based on Model C. As shown in Fig. 3, the IFT increases with salinity reduction. Therefore, a less carboxylic group should be available at the interface with brine dilution. As a result, as observed in Fig. 3, $-COO^-$ concentration reduces, and the crude oil surface becomes less negatively charged.

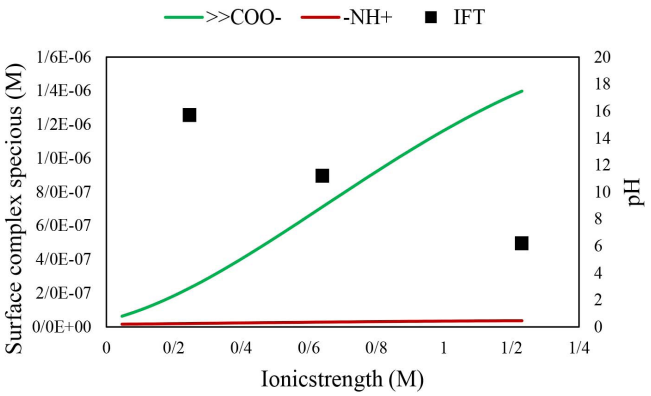

Fig. 3 The concentration of surface complexes based on Model C and the measured crude oil I/brine IFT versus ionic strength for NaCl brine at different salinity levels.

The schematic representation of Fig. 4 provides a more vivid image of the impact of considering the IFT behavior on the electrical properties of crude oil/brine. In the low IFT/high salinity condition (Fig. 4-left), there are more carboxylic acid groups than in the high IFT/low salinity condition (Fig. 4-right). Therefore, as can be observed in Fig. 4, there are more dissociated carboxylic acid groups (-COO-) at low IFT/high salinity conditions. For NaCl brine, the increase in -COOH density opposes and overcomes the effect of EDL shrinkage due to an increase in salinity. Therefore, more NaCl concentration leads to a more negative charge on the crude oil surface. In the case of $NaHCO_3$, IFT remains almost constant with salinity. Fig. 5 compares the predicted ζ potentials of surface complexation models, described in Table 1, plotted against the experimental results of Farhadi et al. [24].

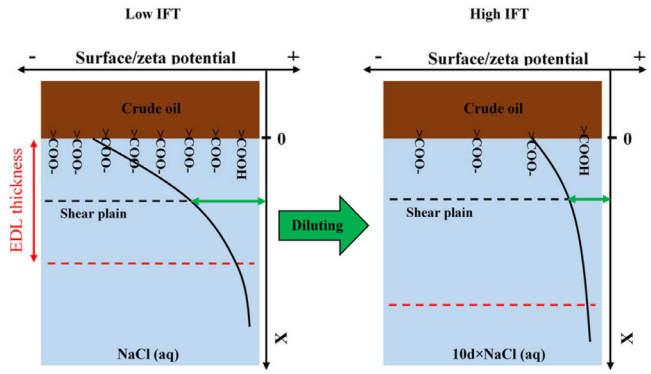

Fig. 4 Schematic representation of the impact of IFT on the surface charge of crude oil/NaCl brine.

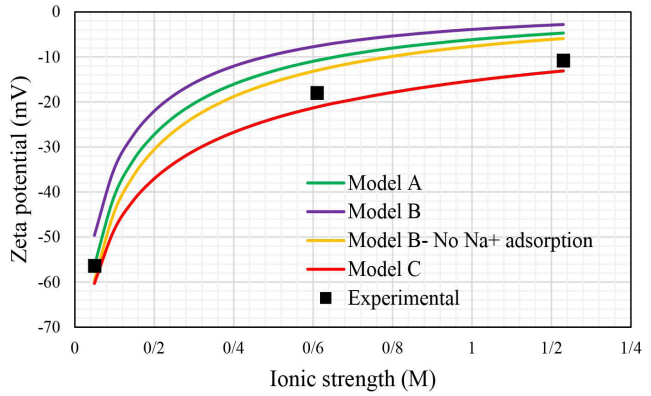

Fig. 5 ζ potential of crude oil I/brine at different salinity levels of $NaHCO_3$ brine.

As shown in Fig. 5, all models can capture the general trend of data. Model B has the worst performance in matching experimental data. However, the same model without Na adsorption (dashed purple line in Fig. 5) provides a good prediction of the experimental ζ potential. Model C performs slightly better than Model B (without Na adsorption). None of the models suggest the Na^+ adsorption on the oil surface. One can conclude that, in the absence of IFT change, all model performs relatively well. Model C provides a better match for the case with slight change in IFT. Also, as shown before, only Model C provides a satisfying performance in the case of major change in IFT. Fig. 6 shows the concentration of surface species formed at the crude oil/$NaHCO_3$ brine interface based on Model C. As shown in Fig. 6, the IFT didn't change significantly with salinity reduction. Therefore, an almost constant carboxylic group number should be available at the interface at different salinity. As a result, as observed in Fig. 6, $-COO^-$ concentration is insensitive to the ionic strength.

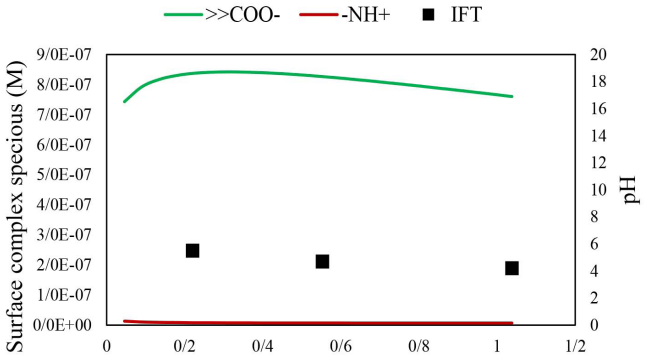

Fig. 6 The concentration of surface complexes based on Model C and the measured crude oil I/brine IFT versus ionic strength for $NaHCO_3$ brine at different salinity levels.

Fig. 7 shows a schematic to explain why salinity reduction significantly decreases the ζ potential. In the case of constant IFT with brine salinity/composition, as discussed before, the -COOH density doesn't change with salinity. In other words, the -COOH density remains constant during a change in $NaHCO_3$ concentration. Also, as concluded, No Na adsorption occurs at the crude oil surface.

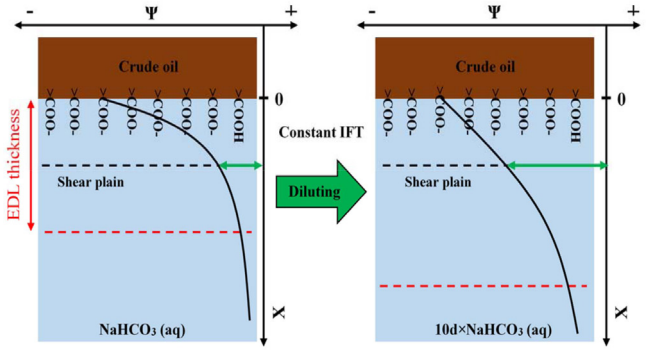

Fig. 7 Schematic representation of the impact of IFT on the surface charge of crude oil/$NaHCO_3$ brine.

However, EDL expands as a result of brine dilution. The EDL expansion reduces the drop in ζ potential with distance from the crude oil surface. In other words, for a more diluted brine sample, the ζ potential is closer to the surface potential. Also, based on Eq. 13, the surface potential per se is a function of ionic strength. In the case of a constant surface charge, a decrease in the brine ionic strength reduces the surface potential. Therefore, the EDL expansion and the reduction in the surface potential, solely due to a decrease in ionic strength, reduce the ζ potential significantly.

Ca^{2+}/Mg^{2+} Concentration

The ζ potentials predicted by the surface complexation models, described in Table 1, were plotted against the experimental results of Farhadi et al. [24] for $CaCl_2$ and $MgCl_2$ brines. As shown in Fig. 8, Model A and Model B predict the general relation between the crude oil/brine ζ potential and ionic strength. However, Model C can match the experimental data in both trend and value.

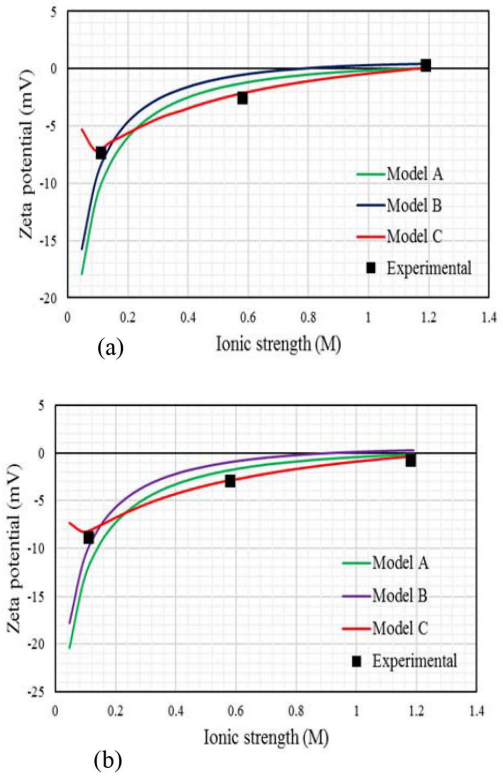

Fig. 8 ζ potential of crude oil I/brine at different salinity levels for: a) $CaCl_2$ brine. b) $MgCl_2$ brine.

Fig. 9 shows the IFT of crude oil/$CaCl_2$ and the concentration of surface complexes based on Model C. As shown in Fig. 9, the equilibrium IFT increases from 4.8 to 11 mN/m by diluting $CaCl_2$ brine from the initial concentration (1.19 M) to 5-time diluted $CaCl_2$ (0.23 M). Therefore, as shown in Fig. 9, fewer carboxylic acid groups are present at the interface at the high IFT/low salinity condition. The change in -COOH density helps us to understand how Model C outperforms Model A and Model B at intermediate and low salinity levels. As described, Model A and Model B assume that -COOH group density doesn't change with brine salinity/composition.

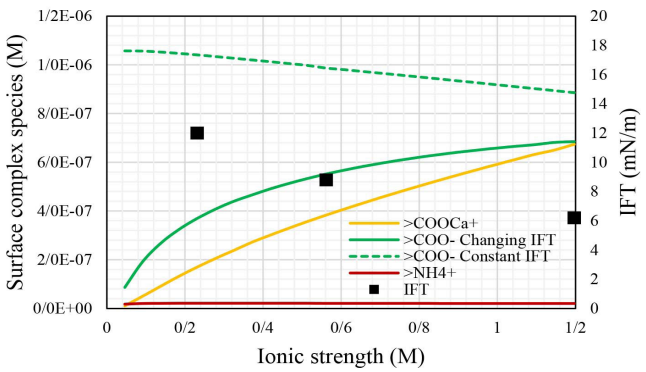

Fig. 9 The concentration of surface complexes based on Model C and the measured crude oil I/brine IFT versus ionic strength for $CaCl_2$ brine at different salinity levels.

Notably, an increase in $CaCl_2$ causes a slight decrease in pH. Therefore, -COOH decreases slightly with an increase in the ionic strength. In other words, these models express that brine dilution slightly increases the -COO-, as depicted in Fig. 9 (dashed green line). However, Model C considers the reduction in Ca^{2+}/Mg^{2+} ions with brine diluting and the decrease in -COO- site density. Therefore, for example, at very low salinity (dashed black box in Fig. 8), Model C shows a higher value for the ζ potential than the other models.

Fig. 10 shows a representative schematic of Model C to describe the electrical behavior in the presence of Ca^{2+}/Mg^{2+} ions. As stated in Fig. 9, the crude oil/brine IFT decreases with increased Ca^{2+} concentration. Therefore, as shown in Fig. 10, more $-COO^-$ sites occupy the oil/brine interface in the case of $CaCl_2$, compared to 10-time diluted $CaCl_2$. Also, adding salinity would result in more Ca^{2+} in the solution, which leads to more absorption of Ca^{2+} on the $-COO^-$ sites. Thus, increasing Ca^{2+} concentration from 10-time diluted $CaCl_2$ to $CaCl_2$ increases the surface and the ζ potential of crude oil/brine from a negative to a positive value.

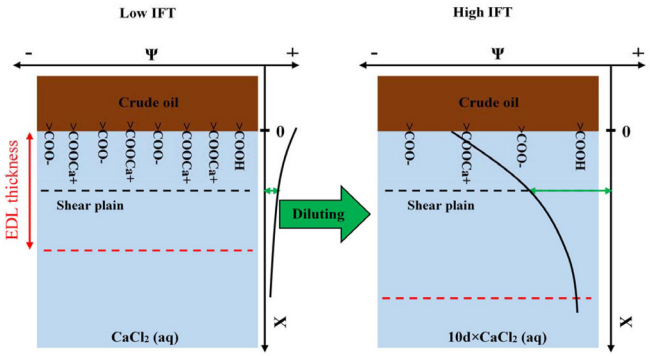

Fig. 10 Schematic representation of the impact of IFT on the surface charge of crude oil/$CaCl_2$ brine.

Conclusions

The current study developed a novel diffuse layer surface complexation model based on the interfacial concentration of surface carboxylic acid. IFT behavior was set as an index to describe the interfacial density of -COOH sites. The model could successfully match the experimental data of the literature better than all previous models. The key findings of this study are as follows:

• Considering the transport of surface-active material from the oil bulk to the oil/brine interface was the main reason behind the developed model's success. Previously, surface

site density was assumed constant, similar to the rock surface. However, using the oil/brine IFT, this study demonstrated that acid (-COOH) cite density is a function of brine salinity and composition.

• The model showed no monovalent ions, Na^+, Cl^-, and SO_4^{2-}, can be adsorbed on the oil/brine interface. The role of these ions in the electrical behavior of crude oil/brine is only to affect the interfacial concentration of -COOH.

• Although Na^+ doesn't adsorb on the oil surface, a reduction in Na concentration led to an increase in the IFT. Therefore, a less carboxylic group would be available at the oil/brine interface. As a result, $-COO^-$ concentration reduces, and the crude oil surface becomes less negatively charged.

• The current study indicated that not only Ca^{2+} and Mg^{2+} are PDIs for a more positively charged interface, but the IFT increase (in this study, for example, by salinity reduction) is another factor that makes the oil/brine interface more positive.

• The model of this study could predict the optimum salinity where the ζ potential is minimum. All previous models state that salinity reduction results in a decrease in the ζ potential. However, the developed model of this study could predict the increase in the ζ potential by further brine dilution after a certain salinity.

• It should be noted that the model considers carboxylic acid as the only surface-active material of the oil bulk. However, basic components can act as surface-active material, too (not in the condition of the current paper). This study suggests that building a comprehensive model to predict the travel of surface-active material from the oil bulk to the interface is the next step to fully predicting the oil/brine interface.

References

1. Al-Shalabi, E. W., & Sepehrnoori, K. (2016). A comprehensive review of low salinity/engineered water injections and their applications in sandstone and carbonate rocks. Journal of Petroleum Science and Engineering, 139, 137–161, doi.org/10.1016/j.petrol.2015.11.027.
2. Austad, T., RezaeiDoust, A., & Puntervold, T. (2010). Chemical mechanism of low salinity water flooding in sandstone reservoirs, SPE Improved Oil Recovery Symposium, doi.org/10.2118/129767-MS.
3. Webb, K., Lager, A., & Black, C. (2008). Comparison of high/low salinity water/oil relative permeability. 29.
4. Sheng, J. J. (2014). Critical review of low-salinity waterflooding, Journal of Petroleum Science and Engineering, 120, 216–224, doi.org/10.1016/j.petrol.2014.05.026.
5. Bartels, W.-B., Mahani, H., Berg, S., & Hassanizadeh, S. (2019). Literature review of low salinity waterflooding from a length and time scale perspective. Fuel, 236, 338–353, doi.org/10.1016/j.fuel.2018.09.018.
6. Bigdeli, A., & Delshad, M. (2023). Strategy for optimum chemical enhanced oil recovery field operation, Journal of Resource Recovery, 1(1), doi:10.52547/JRR.2208.1001.
7. Bigdeli, A., Thyne, G., & Ulyanov, V. (2023). Low salinity water flooding (LSWF), can we move forward? The economic case. Journal of Resource Recovery, 1(1), doi: 10.52547/JRR.2209.1002.
8. Farhadi, H., Rakhodaei, M., Naserian, M., Ayatollahi, S., & Fatemi, M. (2021). Experimental investigation on low salinity effect using dynamic interfacial properties during tertiary water flooding, In 82nd EAGE Annual Conference & Exhibition, 1(1-5), European Association of Geoscientists & Engineers, doi.org/10.3997/2214-4609.202011872.
9. Mahani, H., Keya, A. L., Berg, S., Bartels, W.-B., Nasralla, R., & Rossen, W. R. (2015). Insights into the mechanism of wettability alteration by low-salinity flooding (LSF) in carbonates, Energy & Fuels, 29(3), 1352–1367, doi.org/10.1021/ef5023847.
10. Yousef, A. A., Al-Saleh, S., Al-Kaabi, A., & Al-Jawfi, M. (2010). Laboratory investigation of novel oil recovery method for carbonate reservoirs, Canadian Unconventional Resources and International Petroleum Conference, doi.org/10.2118/137634-MS.
11. Zhang, P., Tweheyo, M. T., & Austad, T. (2007). Wettability alteration and improved oil recovery by spontaneous imbibition of seawater into chalk: Impact of the potential determining ions Ca^{2+}, Mg^{2+}, and SO_4^{2-}, Colloids and Surfaces A: Physicochemical and Engineering Aspects, 301(1–3), 199–208, doi.org/10.1016/j.colsurfa.2006.12.058.
12. Farhadi, H., Ayatollahi, S., & Fatemi, M. (2022). Impact of rock morphology on the dominating enhanced oil recovery mechanisms by low salinity water flooding in carbonate rocks, Fuel, 324, 124769, doi.org/10.1016/j.fuel.2022.124769.
13. Mogharrab, J. M., Ayatollahi, S., & Pishvaie, M. R. (2022). Experimental study and surface complexation modeling of non-monotonic wettability behavior due to change in brine salinity/composition: Insight into anhydrite impurity in carbonates, Journal of Molecular Liquids, 365, 120117, doi.org/10.1016/j.molliq.2022.120117.
14. Dubey, S., & Doe, P. (1993). Base number and wetting properties of crude oils. SPE Reservoir Engineering, 8(03), 195–200, doi.org/10.2118/22598-PA.
15. Mahani, H., Keya, A. L., Berg, S., & Nasralla, R. (2017). Electrokinetics of carbonate/brine interface in low-salinity waterflooding: Effect of brine salinity, composition, rock type, and pH on?-potential and a surface-complexation model. Spe Journal, 22(01), 53–68, doi.org/10.2118/181745-PA.
16. Mazinani, S., Farhadi, H., & Fatemi, M. (2023). Experimental and theoretical investigation of the impact of crude-oil on the wettability behavior of calcite and silicate due to low salinity effect, Fuel, 349, 128608, doi.org/10.1016/j.fuel.2023.128608.
17. Jackson, M. D., Al-Mahrouqi, D., & Vinogradov, J. (2016). Zeta potential in oil-water-carbonate systems and its impact on oil recovery during controlled salinity water-flooding. Scientific Reports, 6(1), 1–13.
18. Sari, A., Xie, Q., Chen, Y., Saeedi, A., & Pooryousefy, E. (2017). Drivers of low salinity effect in carbonate reservoirs. Energy & Fuels, 31(9), 8951–8958, doi.org/10.1021/acs.energyfuels.7b00966.
19. Mahani, H., Keya, A. L., Berg, S., & Nasralla, R. (2017). Electrokinetics of carbonate/brine interface

in low-salinity waterflooding: Effect of brine salinity, composition, rock type, and pH on?-potential and a surface-complexation model, SPE Journal, 22(01), 53–68, doi.org/10.2118/181745-PA.
20. Farhadi, H., Fatemi, M., & Ayatollahi, S. (2021). Experimental investigation on the dominating fluid-fluid and rock-fluid interactions during low salinity water flooding in water-wet and oil-wet calcites, Journal of Petroleum Science and Engineering, 204, 108697, doi.org/10.1016/j.petrol.2021.108697.
21. Mehraban, M. F., Ayatollahi, S., & Sharifi, M. (2019). Role of divalent ions, temperature, and crude oil during water injection into dolomitic carbonate oil reservoirs, Oil & Gas Science and Technology–Revue d'IFP Energies Nouvelles, 74, 36, doi.org/10.2516/ogst/2019003.
22. Farhadi, H., Mahmoodpour, S., Ayatollahi, S., & Fatemi, M. (2023). A novel oil/brine surface complexation model: Capturing the dynamic nature of the interface using IFT, Journal of Molecular Liquids, 123359, doi.org/10.1016/j.molliq.2023.123359.
23. Takeya, M., Shimokawara, M., Elakneswaran, Y., Nawa, T., & Takahashi, S. (2019). Predicting the electrokinetic properties of the crude oil/brine interface for enhanced oil recovery in low salinity water flooding, Fuel, 235, 822–831, doi.org/10.1016/j.fuel.2018.08.079.
24. Kolltveit, Y. (2016). Relationship between crude oil composition and physical-chemical properties, (Master's thesis, The University of Bergen).
25. Mahmoudzadeh, A., Fatemi, M., & Masihi, M. (2022). Microfluidics experimental investigation of the mechanisms of enhanced oil recovery by low salinity water flooding in fractured porous media, Fuel, 314, 123067, doi.org/10.1016/j.fuel.2021.123067.
26. Brady, P. V., Krumhansl, J. L., & Mariner, P. E. (2012). Surface complexation modeling for improved oil recovery, SPE Improved Oil Recovery Symposium, doi.org/10.2118/153744-MS.
27. 27. Qiao, C., Li, L., Johns, R. T., & Xu, J. (2015). A mechanistic model for wettability alteration by chemically tuned waterflooding in carbonate reservoirs, SPE Journal, 20(04), 767–783, doi.org/10.2118/170966-PA.
28. Qiao, C., Johns, R., & Li, L. (2016). Modeling low-salinity waterflooding in chalk and limestone reservoirs, Energy & Fuels, 30(2), 884–895, doi.org/10.1021/acs.energyfuels.5b02456.
29. Takeya, M., Shimokawara, M., Elakneswaran, Y., Okano, H., & Nawa, T. (2019). Effect of acid number on the electrokinetic properties of crude oil during low-salinity waterflooding, Energy & Fuels, 33(5), 4211–4218, doi.org/10.1021/acs.energyfuels.9b00653.
30. Bonto, M., Eftekhari, A. A., & Nick, H. M. (2019). An overview of the oil-brine interfacial behavior and a new surface complexation model, Scientific Reports, 9(1), 1–16.
31. Brady, P. V., & Krumhansl, J. L. (2012). A surface complexation model of oil–brine–sandstone interfaces at 100 C: Low salinity waterflooding, Journal of Petroleum Science and Engineering, 81, 171–176, doi.org/10.1016/j.petrol.2011.12.020.
32. Hiorth, A., Cathles, L., & Madland, M. (2010). The impact of pore water chemistry on carbonate surface charge and oil wettability. Transport in Porous Media, 85(1), 1–21.
33. Sanaei, A., Tavassoli, S., & Sepehrnoori, K. (2019). Investigation of modified Water chemistry for improved oil recovery: Application of DLVO theory and surface complexation model, Colloids and Surfaces A: Physicochemical and Engineering Aspects, 574, 131–145, doi.org/10.1016/j.colsurfa.2019.04.075.
34. Xie, Q., Sari, A., Pu, W., Chen, Y., Brady, P. V., Al Maskari, N., & Saeedi, A. (2018). pH effect on wettability of oil/brine/carbonate system: Implications for low salinity water flooding. Journal of Petroleum Science and Engineering, 168, 419–425, doi.org/10.1016/j.petrol.2018.05.015.
35. Freer, E., & Radke, C. (2004). Relaxation of asphaltenes at the toluene/water interface: Diffusion exchange and surface rearrangement. The Journal of Adhesion, 80(6), 481–496, doi.org/10.1080/00218460490477143
36. Freer, E., Svitova, T., & Radke, C. (2003). The role of interfacial rheology in reservoir mixed wettability. Journal of Petroleum Science and Engineering, 39(1–2), 137–158, doi.org/10.1016/S0920-4105(03)00045-7.
37. Spiecker, P. M., & Kilpatrick, P. K. (2004). Interfacial rheology of petroleum asphaltenes at the oil− water interface. Langmuir, 20(10), 4022–4032, doi.org/10.1021/la0356351.
38. Ayirala, S. C., Al-Saleh, S. H., & Al-Yousef, A. A. (2018). Microscopic scale interactions of water ions at crude oil/water interface and their impact on oil mobilization in advanced water flooding. Journal of Petroleum Science and Engineering, 163, 640–649, doi.org/10.1016/j.petrol.2017.09.054.
39. Farhadi, H., Ayatollahi, S., & Fatemi, M. (2021). The effect of brine salinity and oil components on dynamic IFT behavior of oil-brine during low salinity water flooding: Diffusion coefficient, EDL establishment time, and IFT reduction rate. Journal of Petroleum Science and Engineering, 196, 107862, doi.org/10.1016/j.petrol.2020.107862.
40. Andersson, M., Olsson, M., & Stipp, S. (2014). Predicting the p K a and Stability of Organic Acids and Bases at an Oil–Water Interface. Langmuir, 30(22), 6437–6445, doi.org/10.1016/j.petrol.2020.107862.
41. Czarnecki, J. (2009). Stabilization of water in crude oil emulsions. Part 2. Energy & Fuels, 23(3), 1253–1257, doi.org/10.1021/ef800607u.
42. Yang, F., Tchoukov, P., Pensini, E., Dabros, T., Czarnecki, J., Masliyah, J., & Xu, Z. (2014). Asphaltene subfractions responsible for stabilizing water-in-crude oil emulsions. Part 1: Interfacial behaviors. Energy & Fuels, 28(11), 6897–6904, doi.org/10.1021/ef501826g.
43. Yang, F., Tchoukov, P., Dettman, H., Teklebrhan, R. B., Liu, L., Dabros, T., Czarnecki, J., Masliyah, J., & Xu, Z. (2015). Asphaltene subfractions responsible for stabilizing water-in-crude oil emulsions. Part 2: Molecular representations and molecular dynamics simulations. Energy & Fuels, 29(8), 4783–4794, doi.

org/10.1021/acs.energyfuels.5b00657.
44. Bonto, M., Eftekhari, A. A., & Nick, H. M. (2019). An overview of the oil-brine interfacial behavior and a new surface complexation model. Scientific Reports, 9(1), 1–16.
45. Saeed, M., Jadhawar, P., Zhou, Y., & Abhishek, R. (2022). Triple-layer surface complexation modelling: Characterization of oil-brine interfacial zeta potential under varying conditions of temperature, pH, oil properties and potential determining ions, Colloids and Surfaces A: Physicochemical and Engineering Aspects, 633, 127903, doi.org/10.1016/j.colsurfa.2021.127903.
46. Okasha, T. M., & Alshiwaish, A. (2009). Effect of brine salinity on interfacial tension in Arab-D carbonate reservoir, Saudi Arabia, SPE Middle East Oil and Gas Show and Conference, doi.org/10.2118/119600-MS.
47. Wei, B., Wu, R., Lu, L., Ning, X., Xu, X., Wood, C., & Yang, Y. (2017). Influence of individual ions on oil/brine/rock interfacial interactions and oil–water flow behaviors in porous media, Energy & Fuels, 31(11), 12035–12045, doi.org/10.1021/acs.energyfuels.7b02458.
48. Lashkarbolooki, M., Riazi, M., Ayatollahi, S., & Hezave, A. Z. (2016). Synergy effects of ions, resin, and asphaltene on interfacial tension of acidic crude oil and low–high salinity brines, Fuel, 165, 75–85, doi.org/10.1016/j.fuel.2015.10.030.
49. Eftekhari, A. A., Thomsen, K., Stenby, E. H., & Nick, H. M. (2017). Thermodynamic Analysis of Chalk–brine–Oil Interactions, Energy & Fuels, 31(11), 11773–11782, doi.org/10.1021/acs.energyfuels.7b02019.
50. Buckley, J., Takamura, K., & Morrow, N. (1989). Influence of electrical surface charges on the wetting properties of crude oils, SPE Reservoir Engineering, 4(03), 332–340, doi.org/10.2118/16964-PA.
51. Nenningsland, A. L., Simon, S., & Sjoblom, J. (2010). Surface properties of basic components extracted from petroleum crude oil, Energy & Fuels, 24(12), 6501–6505, doi.org/10.1021/ef101094p.
52. Bertheussen, A., Simon, S., & Sjöblom, J. (2017). Equilibrium partitioning of naphthenic acids and bases and their consequences on interfacial properties, Colloids and Surfaces A: Physicochemical and Engineering Aspects, 529, 45–56, doi.org/10.1016/j.colsurfa.2017.05.068.
53. Freer, E., & Radke, C. (2004). Relaxation of asphaltenes at the toluene/water interface: Diffusion exchange and surface rearrangement, The Journal of Adhesion, 80(6), 481–496, doi.org/10.1080/00218460490477143.
54. Jian, C., Poopari, M. R., Liu, Q., Zerpa, N., Zeng, H., & Tang, T. (2016). Reduction of water/oil interfacial tension by model asphaltenes: The governing role of surface concentration, The Journal of Physical Chemistry B, 120(25), 5646–5654, doi.org/10.1021/acs.jpcb.6b03691.
55. Lashkarbolooki, M., & Ayatollahi, S. (2018). Effects of asphaltene, resin and crude oil type on the interfacial tension of crude oil/brine solution, Fuel, 223, 261–267, doi.org/10.1016/j.fuel.2018.03.029.
56. Brady, P. V., & Krumhansl, J. L. (2012). A surface complexation model of oil–brine–sandstone interfaces at 100 C: Low salinity waterflooding, Journal of Petroleum Science and Engineering, 81, 171–176, doi.org/10.1016/j.petrol.2011.12.020.
57. Drummond, C., & Israelachvili, J. (2004). Fundamental studies of crude oil–surface water interactions and its relationship to reservoir wettability, Journal of Petroleum Science and Engineering, 45(1–2), 61–81, doi.org/10.1016/j.petrol.2004.04.007
58. Hunter, R. J. (2013). Zeta potential in colloid science: Principles and applications, 2, Academic Press.
59. Delgado, Á. V. (2001). Interfacial electrokinetics and electrophoresis, 106, CRC Press.
60. Song, J., Zeng, Y., Wang, L., Duan, X., Puerto, M., Chapman, W. G., Biswal, S. L., & Hirasaki, G. J. (2017). Surface complexation modeling of calcite zeta potential measurements in brines with mixed potential determining ions (Ca^{2+}, CO_3^{2-}, Mg^{2+}, SO_4^{2-}) for characterizing carbonate wettability. Journal of Colloid and Interface Science, 506, 169–179, doi.org/10.1016/j.jcis.2017.06.096.
61. Heberling, F., Trainor, T. P., Lützenkirchen, J., Eng, P., Denecke, M. A., & Bosbach, D. (2011). Structure and reactivity of the calcite–water interface. Journal of Colloid and Interface Science, 354(2), 843–857, doi.org/10.1016/j.jcis.2010.10.047.
62. Sanaei, A., Tavassoli, S., & Sepehrnoori, K. (2019). Investigation of modified Water chemistry for improved oil recovery: Application of DLVO theory and surface complexation model, Colloids and Surfaces A: Physicochemical and Engineering Aspects, 574, 131–145, doi.org/10.1016/j.colsurfa.2019.04.075.
63. Chow, R. S., & Takamura, K. (1988). Electrophoretic mobilities of bitumen and conventional crude-in-water emulsions using the laser Doppler apparatus in the presence of multivalent cations, Journal of Colloid and Interface Science, 125(1), 212–225, doi.org/10.1016/0021-9797(88)90070-7.
64. Healy, T. W., Chan, D., & White, L. (1980). Colloidal behaviour of materials with ionizable group surfaces, Pure and Applied Chemistry, 52(5), 1207–1219, doi.org/10.1351/pac198052051207.
65. Farhadi, H., Mahmoodpour, S., Ayatollahi, S., & Fatemi, M. (2022). Novel experimental evidence on the impact of surface carboxylic acid site density on the role of individual ions in the electrical behavior of crude oil/water, Journal of Molecular Liquids, 362, 119730, doi.org/10.1016/j.molliq.2022.119730.